

Formation of the binary pulsars PSR B2303+46 and PSR J1141–6545

– young neutron stars with old white dwarf companions

Thomas M. Tauris¹ & Thomas Sennels²

¹ Center for High-Energy Astrophysics, University of Amsterdam, Kruislaan 403, NL-1098 SJ Amsterdam, The Netherlands

² Institute of Physics & Astronomy Aarhus University, DK-8000 C, Aarhus, Denmark

Received December 2, 2024

Abstract. We have investigated the formation of the binary radio pulsars PSR B2303+46 and PSR J1141–6545 via Monte Carlo simulations of a large number of interacting stars in binary systems. PSR B2303+46 has recently been shown (van Kerkwijk & Kulkarni 1999) to be the first neutron star – white dwarf binary system observed, in which the neutron star was born *after* the formation of the white dwarf. We discuss the formation process for such a system and are able to put constraints on the parameters of the initial ZAMS binary.

We present statistical evidence in favor of a white dwarf companion to the binary pulsar PSR J1141–6545, just recently discovered in the Parkes Multibeam Survey. In that case this system will be the second one known in which the neutron star was born after its white dwarf companion. We also predict a minimum space velocity of 150 km s^{-1} for PSR J1141–6545, and show it must have experienced an asymmetric SN in order to explain its low eccentricity. Finally, we estimate the birthrate of these systems relative to other binary pulsar systems and present the expected distribution of their orbital periods, eccentricities and velocities.

Key words: binaries: evolution – stars: evolution, mass loss – stars: neutron – white dwarfs: formation – methods: numerical

1. Introduction

Recent observations by van Kerkwijk & Kulkarni (1999) give evidence for a binary (PSR B2303+46) in which the white dwarf was formed before the neutron star (hereafter a WDNS system), as opposed to the normal case in which the neutron star is formed first (NSWD). There are at present ~ 40 systems known in the Galactic disk of the latter case. These are the millisecond pulsar binaries in which an old neutron star was “recycled” via accretion of angular momentum and mass from the giant progenitor of the

white dwarf (e.g. Alpar et al. 1982; van den Heuvel 1984). The third type of compact binaries in which a pulsar has been detected, is the double neutron star systems (NSNS). There are at least 6 of these systems known (Nice, Sayer & Taylor 1996; Manchester et al. 1999). It is the formation of WDNS systems which is of interest in this paper. For a review on the formation and evolution of binary pulsars in general, see Bhattacharya & van den Heuvel (1991).

Millisecond pulsars in the NSWD systems are characterized by short rotational periods ($P_{\text{spin}} < 90 \text{ ms}$) and relatively weak surface magnetic fields ($B < 10^{10} \text{ G}$) and are therefore fairly easy to distinguish observationally from young non-recycled pulsars expected to be found in the WDNS systems. Furthermore, one expects the NSWD systems to have circular orbits ($e \ll 0.1$) since tidal forces will have circularized the orbit very efficiently in the final mass-transfer process (Verbunt & Phinney 1995) – as opposed to the high eccentricities expected in systems where the last formed degenerate star is a neutron star born in a supernova explosion (Hills 1983).

However, it is difficult to determine from radio pulses alone whether an observed non-recycled pulsar belongs to a WDNS system, or if it is the last formed neutron star in a NSNS system. The reason for this is the unknown inclination angle of the binary orbital plane, with respect to the line-of-sight, which allows for a wide range of possible solutions for the mass of the unseen companion. This is why PSR B2303+46 was considered as a candidate for a double neutron star system since its discovery (Stokes, Taylor & Dewey 1985). Only an optical identification of the companion star could determine its true nature (van Kerkwijk & Kulkarni 1999). The very recently discovered non-recycled binary pulsar PSR J1141–6545 (Manchester et al. 1999) has a massive companion in an eccentric orbit ($M_2 \geq 1.0 M_{\odot}$ and $e = 0.17$). This system must therefore be a new candidate for a WDNS system. Only a deep optical observation will be able to distinguish it from the NSNS alternative.

The identification of PSR B2303+46 as a WDNS binary is very important for understanding binary evolu-

tion, even though its existence already had been predicted by most binary population synthesis codes. Below we will demonstrate how to form a WDNS system and put constraints on the initial parameters of the progenitor of PSR B2303+46.

In Section 2 we briefly introduce our evolutionary code, and in Section 3 we outline the formation of a WDNS binary. In Section 4 we discuss our results and in Section 5 we compare with observations of PSR B2303+46 and PSR J1141–6545. The conclusions are summarized in Section 6.

2. A brief introduction to the population synthesis code

Monte Carlo simulations on a large ensemble of binary systems enables one to examine the expected characteristics of a given binary pulsar population and the physics behind the interactions during their evolution. We have used an updated version of the numerical population synthesis code used by Tauris & Bailes (1996). This code follows the evolution of a binary system from the zero-age main sequence (ZAMS) to its “final” state, at all stages keeping careful track of the mass and orbital separation of the two stars. A large number of outcomes is possible from massive binary evolution (see Dewey & Cordes 1987) ranging from systems which merged in a common envelope or became disrupted at the time of the supernova explosion, to binary pulsars with white dwarf, neutron star or black hole companions. In these computations we restrict our attention to systems which are likely to form WDNS binaries.

To simulate the formation of WDNS binaries, we assume that the initial system consists of two ZAMS stars in a circular orbit. In our code we used a flat logarithmic initial separation distribution ($\Gamma(a) \propto a^{-1}$) and assumed a Salpeter initial mass function for the ZAMS primary stellar masses of $N(m) \propto m^{-2.35}$ combined with a mass-ratio function: $f(q) = 2/(1+q)^2$ (Kuiper 1935). We adopt the term “primary” to refer to the *initially* more massive star, regardless of the effects of mass transfer or loss as the system evolves.

In our simulations we used interpolations of the evolutionary grids of Maeder & Meynet (1988, 1989) for initial masses below $12 M_{\odot}$. These grids take into account stellar-wind mass loss in massive stars and giant-branch stars, and also include a moderate amount of overshooting from the convective core. For helium stars, we used the calculations of Paczynski (1971). From these models of stellar evolution we estimate the radius and age of the primary star at the onset of the mass transfer. Using other models with different chemical composition and convective overshooting may have changed these values slightly, but would not have had any significant effect on the parameters of the final population of WDNS systems. We refer to Tauris & Bailes (1996) and Tauris (1996) for a

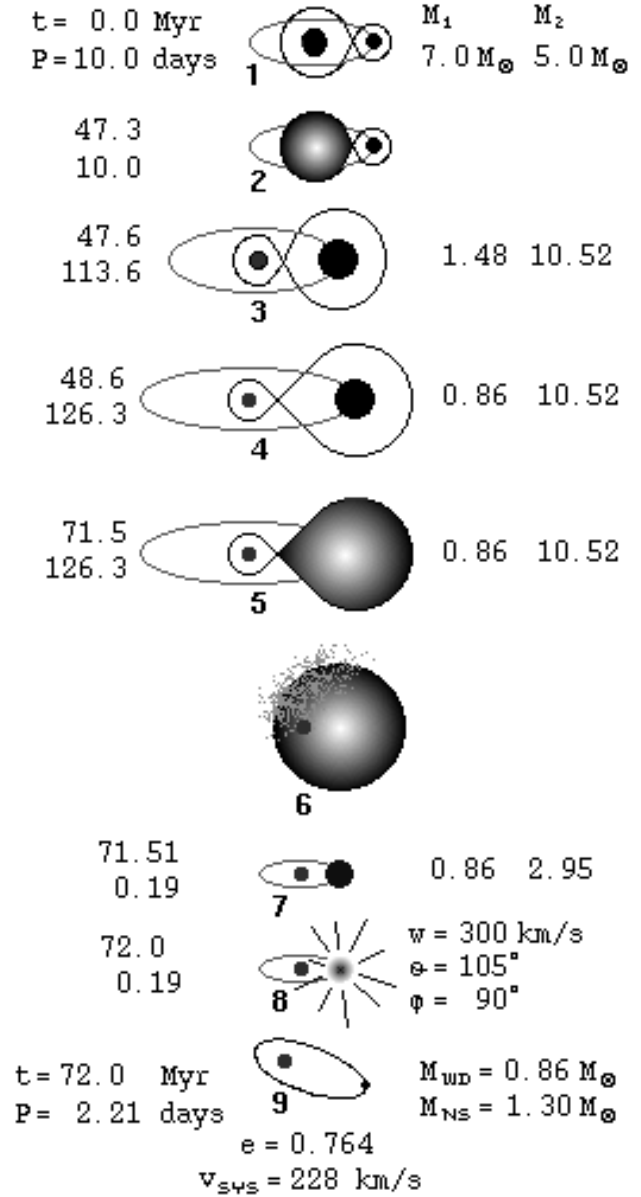


Fig. 1. Illustration of the formation of a typical WDNS system. The neutron star is formed last and is therefore not recycled – see text.

more detailed description of the binary interactions and the computer code.

3. Formation of a white dwarf – neutron star binary

In Fig. 1 we depict the scenario for making a WDNS system and in Fig. 2 we have shown the masses of the initial ZAMS stars which evolve to form WDNS systems. The allowed parameter space is constrained by 4 boundaries described below. In order to successfully form a WDNS system we found it necessary to choose primary masses, M_1

in the interval $5 - 11 M_{\odot}$, secondary masses, M_2 between $3 - 11 M_{\odot}$, and initial separations, a_0 between $5 - 600 R_{\odot}$. In order for the primary to end its life as a white dwarf we must require $M_1 < 11 M_{\odot}$ (cf. boundary I in Fig. 2). On the other hand a minimum mass of $\sim 5 M_{\odot}$ is needed for the primary, since it has to transfer sufficiently mass to the secondary (which is initially lighter than the primary) in order for the latter to explode in a supernova (SN) once its nuclear burning has ceased. As a result of the essential mass accretion onto the secondary, the progenitor binary can not evolve through a common envelope (CE) in the first phase of mass transfer (cf. stage 2 in Fig. 1). The reason is that the timescale for the CE-phase is very short ($10^3 - 10^4$ yr) compared to the duration of a dynamically stable Roche-lobe overflow (RLO) which lasts for ~ 1 Myr. We assumed the RLO to be conservative (*i.e.* total mass and orbital angular momentum remains constant). In order to avoid a CE-phase we required $q = M_2/M_1 > 0.4$ (cf. boundary II in Fig. 2). Hence M_2 is constrained from this requirement in combination with: $M_2 + \Delta M_{\text{RLO}} > M_{\text{SN}}^{\text{crit}}$, where $M_{\text{SN}}^{\text{crit}}$ is the threshold mass for undergoing a supernova explosion and ΔM_{RLO} is the amount of matter accumulated by the secondary from the primary star during the RLO, cf. boundary III in Fig. 2. $M_{\text{SN}}^{\text{crit}}$ is typically $9 - 11 M_{\odot}$ but depends on its core mass, $M_{\text{He}}^{\text{crit}}$ and its evolutionary status at the onset of the mass transfer. It should therefore be noted that the boundaries in Fig. 2 depend on P_{orb} since the evolutionary status of a donor star is important in order to determine $M_{\text{He}}^{\text{crit}}$. Also the onset criterion for the formation of a CE depends on the evolutionary status of the Roche-lobe filling star. The last boundary (IV) in Fig. 2 is the trivial requirement defining the secondary star initially having $M_2 < M_1$.

After the primary star has lost its envelope to the secondary, the helium core will eventually settle as a white dwarf (stage 3 and 4, respectively in Fig. 1). To calculate the final mass of the CO (O-Ne-Mg) white dwarf we assumed:

$$M_{\text{WD}} = \begin{cases} M_{\text{1He}} & M_{\text{1He}} < 0.45 M_{\odot} \\ 0.27 M_{\odot} + 0.40 M_{\text{1He}} & M_{\text{1He}} > 0.45 M_{\odot} \end{cases} \quad (1)$$

(unless $M_{\text{1He}} > M_{\text{He}}^{\text{crit}}$ in which case the mass of primary helium core is above the threshold limit $\sim 2.5 M_{\odot}$ and it collapses in a supernova leaving behind a neutron star remnant).

The subsequent evolution is now reversed. The secondary fills its Roche-lobe and initiates mass transfer onto the white dwarf (stage 5 in Fig. 1). This class of binaries is referred to as cataclysmic variables (CV's) in the literature. Now because of the extreme mass ratio between the secondary star (the donor) and the accreting white dwarf, the orbit will shrink upon mass transfer. Furthermore, if the secondary star is a red giant at this stage (which is almost always the case) it has a deep convective envelope and will expand in response to mass loss. This enhances the mass-transfer rate, which in turn causes the

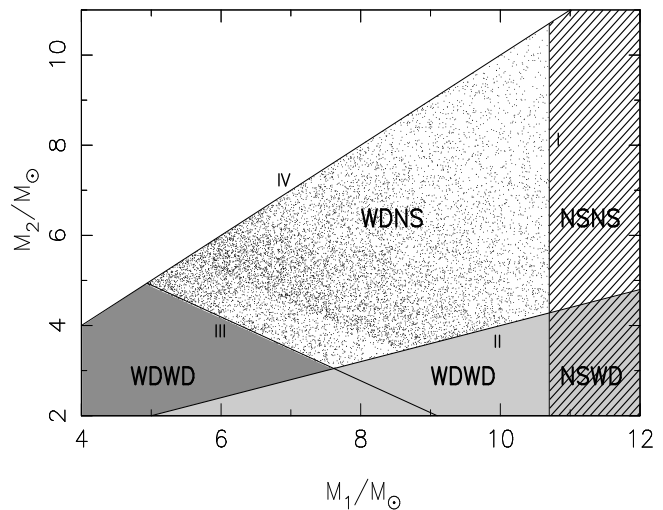


Fig. 2. Area in the ZAMS (M_1, M_2) plane with progenitor systems for WDNS binaries – see text for a discussion.

orbit to shrink faster. This leads to a run-away event and the transferred material piles up and is heated in a cloud around the white dwarf. The white dwarf will be embedded in a CE with the secondary star. In this dynamically unstable situation drag forces causes the white dwarf to spiral-in toward the core of the giant companion (stage 6 in Fig. 1). In this process orbital energy is converted into kinetic energy which provides outward motion and possibly ejection of the envelope. Here we assumed an efficiency parameter of $\eta_{\text{CE}} = 2.0$ (Iben & Livio 1993). If there is not enough orbital energy available to expel the envelope (*i.e.* the binary is too tight), the result is that the white dwarf will merge with the core of the giant – perhaps leading to a type Ia SN and total disruption of the binary (in any case we terminated our calculations for binaries with merging stars). This puts some constraints on the orbital separation at the moment of mass transfer. If the envelope is ejected successfully (stage 7), the helium core will collapse after a short while and explode in a type Ib/c supernova (stage 8). There is plenty of evidence from observations (e.g. Lyne & Lorimer 1994; Tauris et al. 1999) that a momentum kick is imparted to newborn neutron stars. This is probably due to some asymmetry in the neutrino emission driving the explosion. We assumed an isotropic kick direction and used a Gaussian distribution for its magnitude with a mean value, $\langle w \rangle = 500 \text{ km s}^{-1}$ and standard deviation, $\sigma = 200 \text{ km s}^{-1}$. We assumed the neutron star to be born with a mass of $M_{\text{NS}} = 1.3 M_{\odot}$. Given the pre-SN separation and the masses of the exploding helium star and its white dwarf companion, as well as the kick magnitude and direction, we are able to calculate the final orbital period, P_{orb} and eccentricity, e of the WDNS system (cf. stage 9 in Fig. 1).

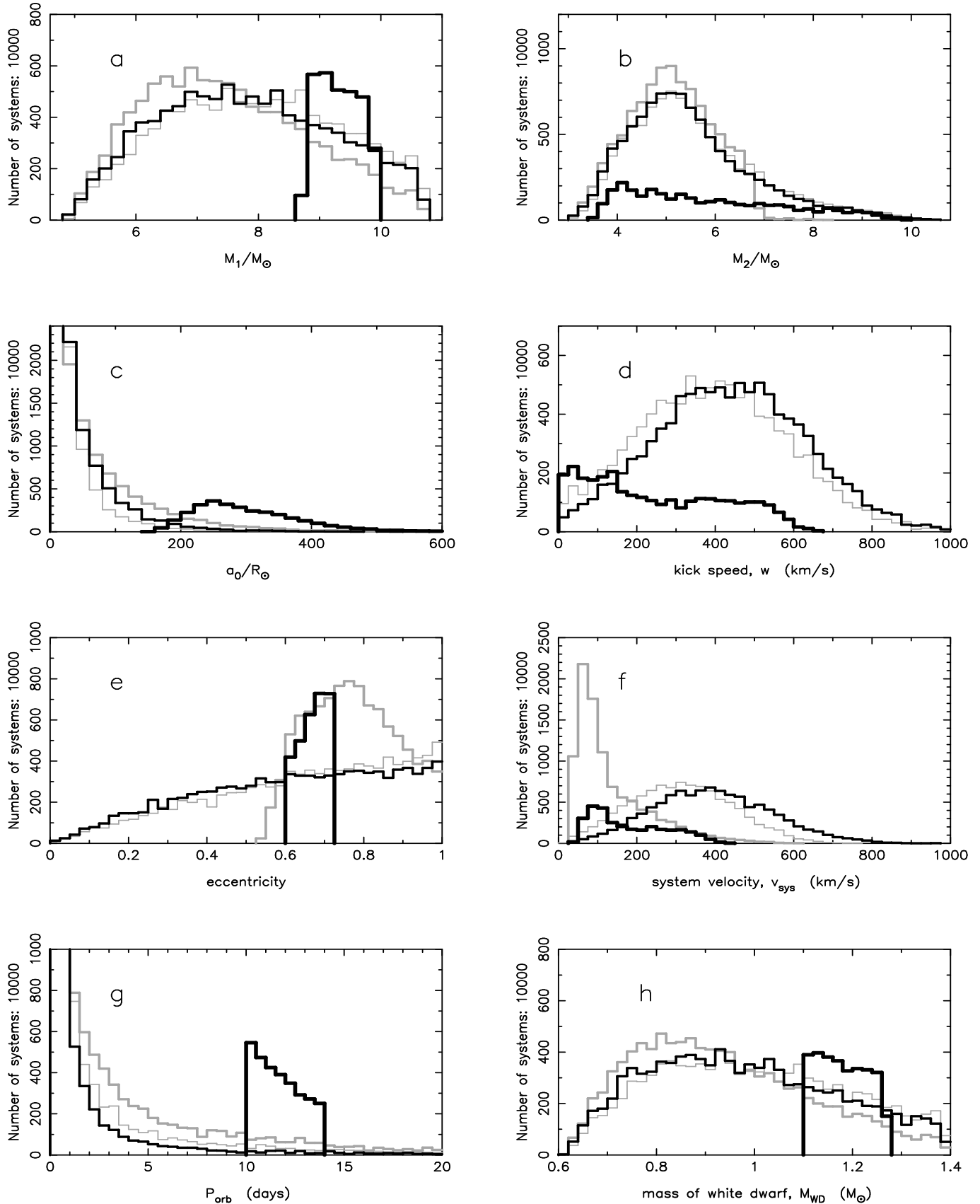


Fig. 3. Distributions of parameters for the initial ZAMS systems (panels a–c) which evolved to form WDNS binaries. The final parameters of these WDNS systems are plotted in panels e–h. See text for further explanation of the different curves.

4. Results

The results of our computations are summarized in Fig. 3 which shows distributions of the parameters of both the ZAMS progenitor binaries (panels a–c) and the observable parameters of the final WDNS binaries (panels e–h). Each panel shows four different distributions of a given parameter for 10 000 systems which successfully evolved to a WDNS binary. These distributions are represented by a black, gray, thin gray and thick black histogram, respectively.

4.1. The black curve: asymmetric SN

The black curve represents our standard simulation where we assumed $\langle w \rangle = 500 \text{ km s}^{-1}$, with $\sigma = 200 \text{ km s}^{-1}$, for the magnitude of kicks in the SN, and a CE efficiency parameter of $\eta_{\text{CE}} = 2.0$. We now describe the distribution of parameters represented by this black curve in each panel.

From panels a–c we conclude that in order to form a WDNS binary one must have a ZAMS binary with $4.9 < M_1/M_\odot < 10.8$, $3.0 < M_2/M_\odot < 10.8$ and $a_0 < 600 R_\odot$. We note that the distribution of kicks in panel d closely follows our assumed input distribution (which is somewhat unknown ad hoc – see e.g. Hartman et al. 1997 for a discussion). It is also seen that the distribution of kicks imparted in binaries which form bound WDNS systems is slightly shifted towards smaller values compared to the trial distribution (*i.e.* on average the WDNS systems have received a kick of $439 \text{ km s}^{-1} \neq 500 \text{ km s}^{-1}$). The reason is simply that, on average, a system has a higher probability of surviving the SN if the kick is small. The maximum kick possible in the SN appears to be 1000 km s^{-1} . However, this is an artifact from our trial distribution of kicks. Applying unlimited values for the magnitude of the kicks it is in principle possible to form a WDNS system using a kick, $w > 1700 \text{ km s}^{-1}$ – resulting in space velocities of $v_{\text{sys}} > 1300 \text{ km s}^{-1}$.

The expected orbital parameters of the formed WDNS systems are shown in panels e–h. The WDNS systems can be formed with any eccentricity, e – though the distribution increases monotonically with increasing values of e . The simulated systemic 3-D velocities of the WDNS systems (panel f) are simply correlated to the distribution of kicks. When comparing with future observations of 2-D transverse velocities one has to multiply this simulated 3-D distribution by a factor of $\pi/4$ in order to separate out the unknown radial velocities.

The distribution of orbital periods, P_{orb} of the WDNS binaries is highly concentrated towards small values of P_{orb} (notice we have not shown the first two bins of the distribution in panel g, which reach values of 6500 and 1100, respectively). This is also seen in Fig. 4 where we have plotted the eccentricity versus the final orbital period for the simulated WDNS systems. The cumulative probability curve for P_{orb} is also shown in the figure. The distribution

of calculated white dwarf masses (in panel h of Fig. 3) is seen to be in the interval $0.6 < M_{\text{WD}}/M_\odot < 1.4$.

We will now briefly describe what happens when we choose other input distributions governing the two most important binary interactions: the SN and the preceding CE-phase.

4.2. The gray curve: symmetric SN

The gray curve in each panel shows the distribution of a given parameter assuming a purely symmetric SN. This assumption apparently does not significantly change the distributions of initial parameters for the binaries ending up as WDNS systems. It has only a moderate effect on the distribution of M_2 and M_{WD} (leading to slightly lower values), but a more significant effect on a_0 and the distribution of final P_{orb} , which tend to be higher without the asymmetry in the SN. This is expected, since in the cases where a kick is added on top of the effect of sudden mass loss, the pre-SN orbit must, on average, be more tight in order to survive the SN. However, most important differences are seen in the distributions of the eccentricity and the systemic velocity. The shift to smaller values for the latter distribution (the mean value of v_{sys} decreases from 393 to 137 km s^{-1}) follows naturally, since now $w = 0$ and v_{sys} is therefore only arising due to the sudden mass loss in the SN.

In the case of post-SN eccentricities, we now only form WDNS systems with $e > 0.5$. The existence of a minimum eccentricity for systems undergoing a symmetric SN follows from celestial mechanics (e.g. Flannery & van den Heuvel 1975):

$$e = \frac{M_{2\text{He}} - M_{\text{NS}}}{M_{\text{WD}} + M_{\text{NS}}} \quad (2)$$

Since we have $M_{2\text{He}} > M_{\text{He}}^{\text{crit}} \simeq 2.5 M_\odot$ and $M_{\text{WD}}^{\text{max}} < 1.4 M_\odot$ it follows that $e > 0.45$.

Another proof of asymmetric SN in nature would therefore be a future detection of a WDNS system with $e < 0.45$ (cf. discussion on PSR J1141–6545 in Section 5.2). The reason why asymmetric SN can result in more circular orbits is a result of the expected randomness in the direction of the kicks. Hence a system which would otherwise have been highly eccentric after a symmetric SN (*i.e.* due to the effect of sudden mass loss alone) can end up being almost circular when momentum is imparted to the newborn neutron star in a particular direction.

It should be noted that the post-SN orbits of the WDNS systems will not circularize later on, since tidal effects are insignificant in systems with two degenerate stars. Only in binaries with $P_{\text{orb}} < 0.6$ days will the orbit circularize in less than a Hubble-time – mainly as a result of general relativistic effects (Shapiro & Teukolsky 1983).

4.3. The thin gray curve: high efficiency in ejection of the CE

The thin gray line in each panel shows a given distribution assuming $\eta_{\text{CE}} = 8.0$. This is a radical change in the efficiency of ejecting the envelope. The efficiency of converting orbital energy into kinetic energy, which expels the envelope, is defined by: $\Delta E_{\text{bind}} \equiv \eta_{\text{ce}} \Delta E_{\text{orb}}$ (Webbink 1984), or:

$$\frac{GM_2 M_2^{\text{env}}}{\lambda a_i r_L} = \eta_{\text{ce}} \left[\frac{GM_{\text{WD}} M_{2\text{He}}}{2a_f} - \frac{GM_{\text{WD}} M_2}{2a_i} \right] \quad (3)$$

which yields the following change in orbital separation:

$$\frac{a_f}{a_i} = \frac{M_{\text{WD}} M_{2\text{He}}}{M_2} \frac{1}{M_{\text{WD}} + 2M_{2\text{env}}/(\eta_{\text{ce}} \lambda r_L)} \quad (4)$$

where $r_L = R_L/a_i$ is the dimensionless Roche-lobe radius of the donor star, λ is a weighting factor (≤ 1.0) for the binding energy of the core and envelope of the donor star and, finally, where $M_{2\text{He}}$, $M_{2\text{env}}$, a_i and a_f are the mass of the core and hydrogen-rich envelope of the evolved companion star, and the pre-CE and post-CE separation, respectively. We notice that this large change in η_{CE} barely changes our results. The thin gray curve seems to follow the black curve closely in most of the panels. Only the final P_{orb} are higher in this case – though the shape of the distribution remains the same. This result is expected since in this case the envelope is ejected more easily in the CE, resulting in larger pre-SN separations. One can easily show that roughly speaking: $(a_f/a_i) \propto \eta_{\text{CE}}$ and hence we expect the pre-SN binaries to have much wider orbits in the case where $\eta_{\text{CE}} = 8.0$ (by a factor of 4). However, many of the wide pre-SN binaries do not survive the SN, so the overall final P_{orb} distribution only differs slightly from the case with $\eta_{\text{CE}} = 2.0$. This also explains why the selected w and resulting v_{sys} are slightly lower, since binaries are more easily disrupted having wider orbits. Thus w and v_{sys} of the binaries which do survive the SN are smaller in this case where $\eta_{\text{CE}} = 8.0$.

We also experimented with different initial mass functions (IMF) but conclude that our simulated results for the WDNS systems are quite robust against changes in the IMF or the initial separation function for a_0 (see below).

5. Comparison with observations

The observed parameters of the binary radio pulsars PSR B2303+46 and PSR J1141–6545 are given in Table 1.

5.1. PSR B2303+46

Knowing the observed parameters for the orbital period, eccentricity and mass function, f we have investigated which initial ZAMS binaries would form a system like PSR B2303+46 and also constrained its systemic velocity. The distribution of parameters for 3000 WDNS sys-

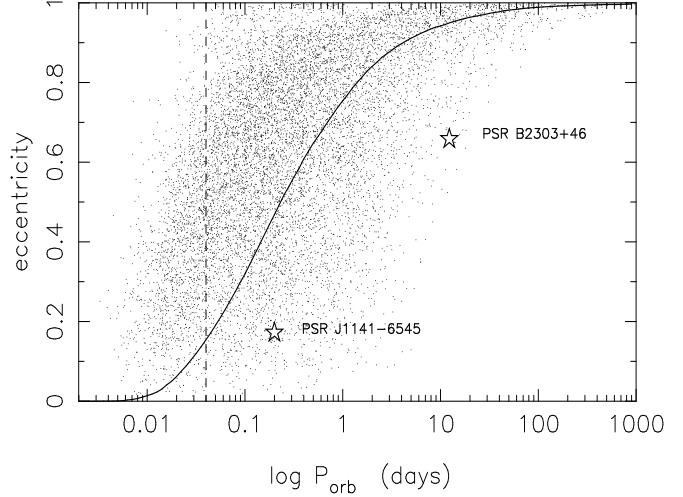


Fig. 4. Eccentricity versus final orbital period for the simulated WDNS systems. The curve gives the probability that P_{orb} for a simulated WDNS system is less than the corresponding value on the x-axis. We assumed here $\langle w \rangle = 500 \text{ km s}^{-1}$, $\sigma = 200 \text{ km s}^{-1}$ and $\eta_{\text{CE}} = 2.0$. Systems formed to the left of the dashed line will coalesce within $\sim 10 \text{ Myr}$ as a result of gravitational wave radiation.

tems which resemble PSR B2303+46 are shown as the thick black histograms in Fig. 3. We define a WDNS system to resemble PSR B2303+46 if $10 < P_{\text{orb}} < 14 \text{ days}$, $0.60 < e < 0.72$ and $M_{\text{WD}} > 1.1 M_{\odot}$. The minimum white dwarf mass given in Table 1 is obtained from its observed mass function. However a tighter constraint is found in combination with the measurement of the general relativistic rate of periastron advance (Thorsett et al. 1993; Arzoumanian 1995) which yields a solution for the total system mass: $M_{\text{NS}} + M_{\text{WD}} = 2.53 \pm 0.08 M_{\odot}$, and hence $M_{\text{WD}} > 1.20 M_{\odot}$. In order to produce such a high mass for the white dwarf we need a minimum mass $M_1 > 8.8 M_{\odot}$ for its progenitor, but notice that the wide range of possible secondary masses remains.

The most distinct feature of PSR B2303+46 is its very wide orbit: $P_{\text{orb}} = 12.3 \text{ days}$. It is evident from Fig. 4, and panel g in Fig. 3, that such a large value for P_{orb} is very rare. We find that only $\sim 5\%$ of all WDNS systems are formed with $P_{\text{orb}} \geq 12.3 \text{ days}$ (see the cumulative probability curve in Fig. 4). The large observed value of P_{orb} leads to a large initial separation of the ZAMS binaries in the interval: $160 < a_0/R_{\odot} < 600$. To test whether or not the resulting P_{orb} distribution for the WDNS systems simply reflects our initial trial distribution for a_0 (which is flat in $\log a_0$), we tried to run our code with a constant distribution function (*i.e.* all values of a_0 are a priori equally probable). This however, does not change our conclusions and we infer that the distribution of P_{orb} is highly concentrated toward small values.

Table 1. Observed parameters of the WDNS system PSR B2303+46 and the WDNS candidate PSR J1141–6545. We use $M_{\text{NS}} = 1.3 M_{\odot}$.

PSR	P_{orb}	f	$M_{\text{WD}}^{\text{min}}$	ecc.	P_{spin}	\dot{P}_{spin}
B2303+46	12.3	0.2464	1.13	0.658	1066	0.57
J1141–6545	0.198	0.1774	0.97	0.172	394	4.31
	days	M_{\odot}	M_{\odot}		ms	10^{-15}

For the expected value of the recoil velocity of PSR B2303+46 we find it must be in the interval: $50 < v_{\text{sys}} < 440 \text{ km s}^{-1}$, with a mean value of 181 km s^{-1} .

5.2. PSR J1141–6545

This interesting binary radio pulsar was recently found in the ongoing Parkes Multibeam Survey (Manchester et al. 1999). The high value of \dot{P}_{spin} in combination with its relatively slow rotation rate ($P_{\text{spin}} = 394 \text{ ms}$) and non-circular orbit ($e = 0.17$) identifies this pulsar as being young and the last formed member of a double degenerate system. Given $P_{\text{orb}} = 0.198 \text{ days}$ it is also evident that a non-degenerate star can not fit into the orbit without filling its Roche-lobe. The minimum companion mass of $0.97 M_{\odot}$ (assuming $M_{\text{NS}} = 1.3 M_{\odot}$) and its location in the (P_{orb}, e) diagram makes this binary a good candidate for a WDNS system. We note, that $P_{\text{orb}} = 0.198 \text{ days}$ is right at the mean value of the simulated distribution – though the eccentricity is lower than average for this orbital period. We must however, beware of selection effects at work here. It is well known that it is much more difficult to detect a periodic signal emitted from an accelerated pulsar in a narrow orbit compared to a wide orbit (Ramachandran 1999). It is therefore expected that future detections of WDNS systems will fill up mainly the area to the right side of the curve in Fig. 4. Although some WDNS systems should be found in very tight orbits from improved future acceleration searches, it should also be noted that tight binaries cannot avoid merging as a result of emission of gravitational waves (Landau & Lifshitz 1958) on a timescale given by (Tauris 1996): $\tau_{\text{gwr}} = 1/8 \times |J_{\text{orb}}/\dot{J}_{\text{gwr}}|$, or:

$$\tau_{\text{gwr}} = \frac{(a/R_{\odot})^4}{M_{\text{WD}} M_{\text{NS}} (M_{\text{WD}} + M_{\text{NS}})/M_{\odot}^3} 1.5 \times 10^8 \text{ yr} \quad (5)$$

where a is the post-SN separation found from Kepler’s 3. law:

$$a/R_{\odot} = \left[(P_{\text{orb}}/\text{days}) 8.626 \sqrt{(M_{\text{WD}} + M_{\text{NS}})/M_{\odot}} \right]^{2/3} \quad (6)$$

Given the values of P_{orb} and $M_{\text{WD}}^{\text{min}}$, PSR J1141–6545 will merge within $\sim 640 \text{ Myr}$ (a spectacular event for LIGO).

However, the average lifetime of a non-recycled pulsar is only $\sim 10 \text{ Myr}$ (Taylor, Manchester & Lyne 1993). In Fig. 4 we have shown with a vertical dashed line WDNS systems which will merge on a timescale of $\sim 10 \text{ Myr}$. Hence all binaries found to the left of this line ($P_{\text{orb}} \lesssim 1 \text{ hr}$) are most likely to coalesce within the lifetime of the observed radio pulsar.

As shown in Section 4.2 we conclude that the SN forming the observed pulsar in PSR J1141–6545 must have been asymmetric, given the low eccentricity of the system. We find a minimum kick of 100 km s^{-1} necessary to reproduce $e = 0.17$ for a system with similar P_{orb} . More interesting, we are able to constrain the minimum space velocity of PSR J1141–6545, and we find: $v_{\text{sys}} > 150 \text{ km s}^{-1}$. A future proper motion determination and a possible detection of a spectral line from the white dwarf will be able to verify this result.

5.3. On the relative formation rates of WDNS, NSNS and NSWD systems and the nature of PSR J1141–6545

We have used our population synthesis code to generate a large number of compact binaries using wide initial trial distributions for the ZAMS binaries. In Table 2 we show the relative formation rates of these systems (normalized to the number of trial simulations). The remaining binaries either evolved into WDWD systems, coalesced, became disrupted in a SN or formed a black hole binary. It should be noted that many of the parameters governing the binary interactions are not very well known, and that the relative formation rates are sensitive to these parameters. However, the aim of this little exercise is simply to demonstrate it is possible to match the present observations with the results of evolutionary simulations.

To estimate the relative Galactic abundancies of *active* WDNS, NSNS and NSWD binaries, we have weighted each of the formation rates by the observable lifetime of the pulsars, τ_{psr} .

For non-recycled pulsars we chose a lifetime of 10 Myr . For the recycled pulsars τ_{psr} depends on the mass-transfer timescale and the amount of material accreted (and hence on the mass of the progenitor of the last formed degenerate star). The mass transfer causing the recycling in the NSNS systems takes place on a sub-thermal timescale. Hence the rejuvenated \dot{P} is relatively large ($\sim 10^{-18}$) and these pulsars are expected to terminate their radio emission in less than about one Gyr. Hence we chose $\tau_{\text{psr}} = 1000 \text{ Myr}$ for the NSNS binaries with an observed recycled pulsar. The situation is similar for the NSWD systems with heavy CO/O-Ne-Mg white dwarf companions. However, the binary NSWD systems with low-mass helium white dwarf companions are expected to have been recycling over a long interval of time ($\sim 100 \text{ Myr}$) and exhibit long spin-down ages of 5–10 Gyr. We therefore chose an overall average value of $\tau_{\text{psr}} = 3000 \text{ Myr}$ for the NSWD population.

Table 2. Simulated relative formation rates as well as theoretical and observed Galactic disk abundances of WDNS, NSNS and NSWD binaries. The observed globular cluster pulsars are not included since they are formed via exchange collisions in a dense environment.

binary	rel. birthrate	τ_{psr}	N_{sim}	N_{obs}
WDNS	0.00567	10 Myr	1.40	2
NSNS	0.00032	10 Myr	0.08	0
—	—	1000 Myr	7.91	6
NSWD	0.00052	3000 Myr	38.6	40

For these values of τ_{psr} , in combination with our simulated relative birthrates, we find the relative number of such systems expected to be observed, N_{sim} (normalized to the total actual number of binary pulsars detected so far). We see that our simple estimates matches well with the observations – cf. N_{sim} and N_{obs} in columns 4 and 5, respectively in Table 2.

The actual values of τ_{psr} are uncertain, and a weighting factor should also be introduced to correct for the number of different systems merging from gravitational wave radiation. Furthermore, when comparing with observations one must also correct for other important effects, such as the different beaming factors (*i.e.* the area on the celestial sphere illuminated by the pulsar) between recycled and non-recycled pulsars. Slow non-recycled pulsars usually have much more narrow emission beams than those of the recycled pulsars and hence they are more unlikely to be observed. On the other hand their pulse profiles are less likely to be smeared out due to their long pulse periods. There are many selection effects involved here and we have a more rigorous analysis in preparation.

Despite various uncertainties described above one important result can be extracted from our calculations: the expected formation rate of WDNS systems is ~ 16 times higher than that of the NSNS systems. The main reason is that the WDNS binaries only need to survive one SN, and that their progenitors are favored by the IMF. Based on our simulations we therefore conclude that since the pulsar in PSR J1141–6545 is young (non-recycled) it is most likely (at the $\sim 95\%$ confidence level) to have a white dwarf companion. This firm prediction will hopefully be verified soon from optical observations.

6. Conclusions

- We have adapted a numerical computer code to study the formation process of WDNS systems and have demonstrated that many initial ZAMS binary configurations can result in the formation of such systems.
- We have constrained the parameters for the progenitor system of PSR B2303+46.

- We have presented strong evidence in favor of a white dwarf companion (rather than a neutron star) to the newly discovered binary pulsar PSR J1141–6545.
- We have also demonstrated that an applied kick was necessary in the formation scenario of this system.
- Finally, we predict PSR J1141–6545 to have a minimum 3-D systemic velocity, $v_{\text{sys}} > 150 \text{ km s}^{-1}$.

Acknowledgements. We thank Dick Manchester and the Parkes Multibeam Survey team for releasing the orbital parameters of PSR J1141–6545 prior to publication. T.M.T. acknowledges the receipt of a Marie Curie Research Grant from the European Commission.

References

- Alpar M. A., Cheng A. F., Ruderman M. A., Shaham J., 1982, *Nat.* 300, 728
- Arzoumanian Z., 1995; PhD. Thesis, Princeton Uni.
- Bhattacharya D., van den Heuvel E.P.J., 1991, *Phys. Reports* 203, 1
- Dewey R. J., Cordes J. M., 1987, *ApJ.* 321, 780
- Flannery B. P., van den Heuvel E.P.J., 1975, *A&A* 39, 61
- Hartman J. W., Bhattacharya D., Wijers R., Verbunt F., 1997, *A&A* 322, 477
- Hills J., 1983, *ApJ.* 267, 322
- Iben Jr., Livio M., 1993, *PASP* 105, 1373
- Kuiper G. P., 1935, *PASP* 47, 15
- Landau L.D., Lifshitz E., 1958, *The Classical Theory of Fields*, Pergamon Press, Oxford
- Lyne A. G., Lorimer D. R., 1994, *Nat.* 369, 127
- Maeder A., Meynet G., 1988, *A&AS* 76, 411
- Maeder A., Meynet G., 1989, *A&A* 210, 155
- Manchester R. N., Lyne A. G., Camilo F., Kaspi V. M., Stairs I. H., Crawford F., Morris D. J., Bell J. F., D’Amico N., 1999, in preparation
- Nice D. J., Sayer R. W., Taylor J. H., 1996, *ApJ.* 466, L87
- Paczynski B., 1971, *Acta Astron.* 21, 1
- Ramachandran R., 1999, in: 19th Texas Symposium on Relativistic Astrophysics, Paris, eds: J. Paul, T. Montmerle and E. Aubourg (CEA Saclay).
- Shapiro S.L., Teukolsky S.A., 1983, *Black Holes, White Dwarfs and Neutron Stars*, Wiley-Interscience
- Stokes G. H., Taylor J. H., Dewey R. J., 1985, *ApJ.* 294, L21
- Tauris T.M., 1996, *A&A* 315, 453
- Tauris T.M., Bailes M., 1996, *A&A* 315, 432
- Tauris T.M., Fender R. P., van den Heuvel E. P. J., Johnston H. M., Wu K., 1999, *MNRAS* in press
- Taylor J. H., Manchester R. N., Lyne A. G., 1993, *ApJS.* 88, 529
- Thorsett S. E., Arzoumanian Z., McKinnon M., Taylor J. H., 1993, *ApJ.* 405, L29
- van Kerkwijk M. H., Kulkarni S. R., 1999, *ApJ.* 516, L25
- van den Heuvel E. P. J., 1984, *JA&A* 5, 209
- Verbunt F., Phinney E., 1995, *A&A* 296, 709
- Webbink R. F., 1984, *ApJ.* 277, 355